ENCIT 2018

ABCM Associação Brasileira de Engenharia e Ciências Mecânicas

17th Brazilian Congress of Thermal Sciences and Engineering
November 25th-28th, 2018, Águas de Lindóia, SP, Brazil

ENCIT-2018-0121
DESIGN OF TYPICAL COOLING JACKET FOR LIQUID PROPELLANT ROCKET ENGINE BY COMPUTATIONAL FLUID DYNAMICS

Daniel Roberto Ferreira
National Institute of Space Research - Combustion and Propulsion Laboratory
Rodovia Presidente Dutra km 40, Cachoeira Paulista, SP, Brazil, cep 12630-000.
daniel.ferreira@inpe.br

Wladimyr Mattos da Costa Dourado
Institute of Aeronautic and Space - Space Propulsion Division
Praça Marechal Eduardo Gomes 50, Vila das Acácias, São José dos Campos, SP, Brazil, cep 12228-904.
wladimyrwmcd@iae.cta.br

Abstract. *This paper presents a study of typical cooling jacket for liquid propellant rocket engine (LPRE). Initially semi-empirical calculation was performed, to specify the boundary conditions of heat flux provide by combustion. Posteriorly the temperatures of walls and pressure drop on the cooling jacket were calculated. The geometry and mesh of the cooling jacket were design on parametric software and then analysed the conjugate heat transfer in OpenFOAM CFD software, with the same boundary conditions considered on semi-empirical calculation. The results of numerical and semi-empirical calculation achieved were confronted. Finally it were possible to correct the semi-empirical calculation, according to proposed literature, considering that numerical calculation returned the reliable result and next of experimental analysis. This study is the first step to align the semi-empirical calculation with CFD modeling. The next step will be align both with experimental study. The confront this results possible close the cycle of the modern engineering approach, creating a strength tool of thermal analysis applied on liquid propellant rocket engine.*

Keywords: *Liquid Propellant Rocket Engine, Regenerative Cooling, Cooling Jacket, CFD (Computational Fluid Dynamics), Conjugate Heat Transfer.*

1. INTRODUCTION

In liquid propellant rocket engines (LPRE) the most commonly used cooling method is called regenerative cooling. In this method, usually the propellant is the fuel that flows between the inner and outer walls of the combustion chamber. The walls are connected by ribs and thus form the cooling jacket (Sutton and Biblartz, 2001). Cooling is designed to minimize wall temperatures and prevent engine collapse. Therefore, the flow and dimensions of the jacket should be carefully determined (see Fig. 1) (NASA, 1972).

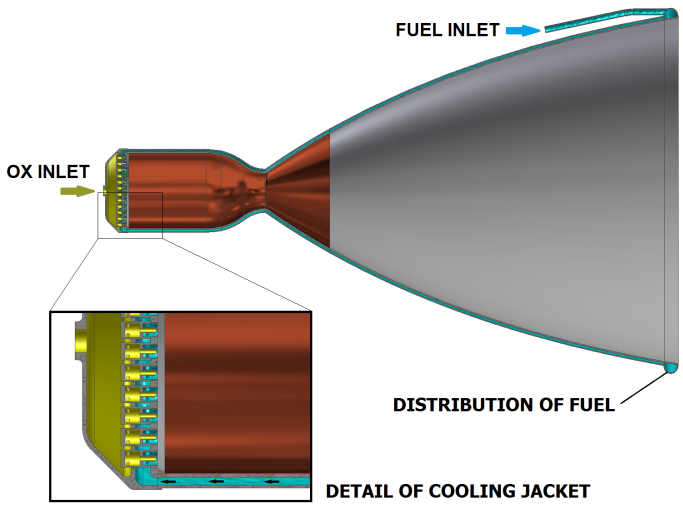

Figure 1. Cooling jacket scheme

The numerical study of this system is performed through conjugated heat transfer analysis, which occurs when there is the coupling of two or more domains subject to a heat flow.

The objective of this study is to perform a CFD modeling of the cooling jacket and compare with the semi-empirical solution proposed by Vasiliev *et al.* (1993) and Kessaev (1997). After comparing the solutions, the semi-empirical calculation must be adjust to return results close to CFD solution.

2. METHODOLOGY

Initially an internal profile of a generic combustion chamber was defined that produces thrust of approximately 80 kN. The dimensions of the cooling system channels are based on values proposed by the literature Kessaev (1997). The dimensions are, 4 mm in height of the channel, 2 mm in thickness of internal and external wall, 1 mm for ribs thickness on the throat, total number of ribs 100 (see Fig. 2).

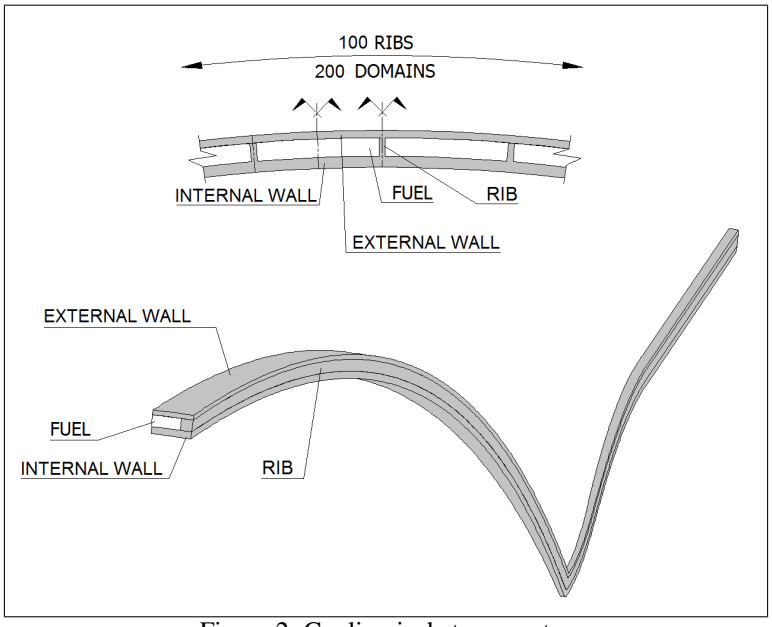

Figure 2. Cooling jacket symmetry

The initial conditions are: temperature equal to $300K$ in all domains, total fuel mass flow rate at the inlet cooling jacket equivalent to $\dot{m} = 8.5\ kg/s$ and static pressure at the output equal to $0\ MPa$. Materials of construction are for internal wall and ribs OFHC copper, for external wall 304 stainless steel and fuel ethanol. It is noteworthy that all thermophysical properties of the domains are constants (μ dynamic viscosity, ρ density, k thermal conductivity and c_p specific heat at constant pressure).

After defined the geometry, materials properties, combustion chemical equilibrium, parameters of design, initial and boundary conditions, theses considerations allows the semi-empirical calculation and CFD can be performed.

2.1 Semi-empirical calculation

2.1.1 Convective heat flux from gas side

Convective heat flux q_{co} provide by combustion gases can be obtained by Eq. 1 (Kessaev, 1997) (Vasiliev *et al.*, 1993).

$$q_{co}(X) = \frac{B\ \ (1-\beta^2)\ \ p_k^{0.85}\ \ S}{\bar{D}^{1.82}\ \ d_g^{0.15}\ \ Pr^{0.58}} \tag{1}$$

Where B is the coefficient of adjustment, β non-dimensional velocity, p_k chamber pressure, $\bar{D}$ non-dimensional diameter, d_g throat diameter, Pr Prandtl number of the hot gas and S is the thermophysical parameter and can be obtained by Eq. 2.

$$S = \frac{(H_{or} - H_{ct})\ \ \mu_{1000}^{0.15}}{R_{or}^{0.425}\ \ T_{or}^{0.32}\ \ (1+T_{ct})^{0.595}\ \ (3+T_{ct})^{0.15}} \tag{2}$$

Where T_{or} is the hot gas temperature at wall layer, T_{ct} inner wall temperature on gas side, H_{or} gas mixture enthalpy at T_{or} temperature, H_{ct} gas mixture enthalpy at T_{ct} temperature, R_{or} specific gas constant for gases mixture at wall layer and μ_{1000} dynamic viscosity of the hot gas at $1000K$.

The B coefficient depends of T_{ct} and γ (ratio of specific heats) values (see Fig. 3).

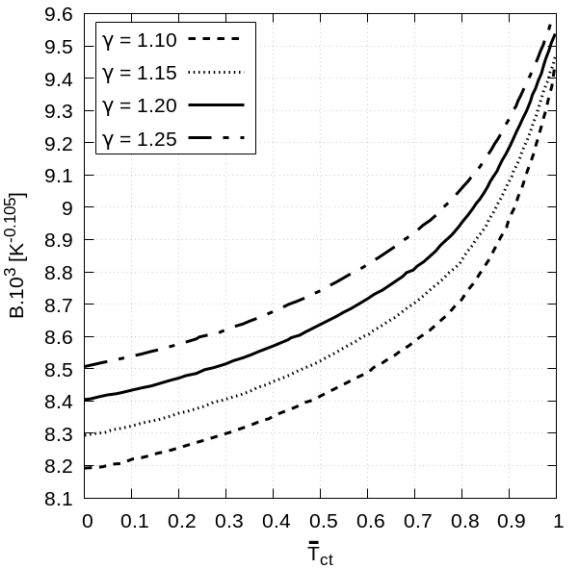

Figure 3. B coefficient

Non-dimensional velocity β is a relation of the maximum velocity of the hot gas in the combustion chamber U_∞ with the maximum velocity possible of the hot gas in the combustion chamber U_{max} and can be expressed in function of the Mach number M from the thermodynamic and isentropic flow through nozzles theory relations (Eq. 3) (Sutton and Biblartz, 2001).

$$\beta = \frac{U_\infty}{U_{max}} \Longrightarrow \beta = \sqrt{1 - \frac{1}{1 + \frac{(\gamma-1)M^2}{2}}} \tag{3}$$

The Mach number M can be expressed in an implicit function of the non-dimensional diameter (Eq. 4) from the area and pressure relations.

$$\bar{D}^2 = \frac{1}{M}\left\{\frac{1 + \left[\frac{(\gamma-1)M^2}{2}\right]}{1 + \left[\frac{(\gamma-1)}{2}\right]}\right\}^{\frac{\gamma+1}{2(\gamma-1)}} \tag{4}$$

Non-dimensional diameter is defined by Eq. 5.

$$\bar{D} = \frac{D(X)}{d_g} \tag{5}$$

Where $D(x)$ is the combustion chamber diameter at X position.

The β coefficient was plotted in function of non-dimensional diameter $\bar{D}$ and are represented on the Fig. 4 for the convergent and divergent regions of the combustion chamber.

2.1.2 Radiation heat flux from gas side

Radiation heat flux q_{rad} provide by combustion gases can be obtained by Eq. 6 (Kessaev, 1997) (Vasiliev *et al.*, 1993).

$$q_{rad} = \epsilon_{wall}\ \epsilon_{gas}\ \varphi\ \epsilon_{rad}\ \left(\frac{T_k}{100}\right)^4 \tag{6}$$

Where T_k is the core chamber temperature and ϵ_{rad} is the emissivity coefficient of the total radiation and has the value of $\epsilon_{rad} = 5.67\frac{W}{m^2K^4}$.

The emissivity coefficients ϵ_{wall}, ϵ_{gas}, φ are estimated according to Kurpatenkov *et al.* (1989) and have values less than 1 (Eq. 7).

$$\epsilon_{wall}\ \epsilon_{gas}\ \varphi\ < 1 \tag{7}$$

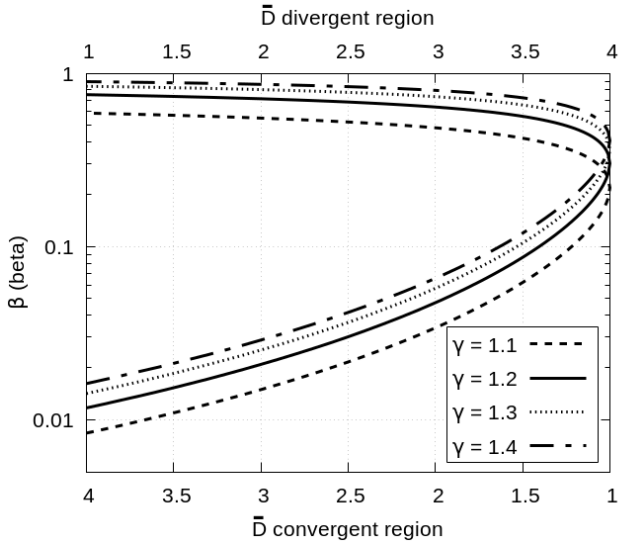

Figure 4. Dimensionless velocity

Distribution $q_{rad}(X)$ along the combustion chamber is estimated by empirical relations for each region. The distribution is in function of the length X and non-dimensional diameter $\bar{D}$ are represented on the next equations:

For the $X = 0$:

$$q_{rad}(0) = 0.25 \;\; q_{rad} \tag{8}$$

On the convergent region for $(\bar{D} < 1.2)$:

$$q_{rad}(X) = q_{rad} \tag{9}$$

On the convergent region for $(1.2 \leq \bar{D} < 1)$:

$$q_{rad}(X) = \left[1 - 12.5\left(1.2 - \bar{D}\right)^2\right] q_{rad} \tag{10}$$

On the throat for $(\bar{D} = 1)$:

$$q_{rad}(X) = 0.5 \;\; q_{rad} \tag{11}$$

On the divergent region for $(\bar{D} > 1)$:

$$q_{rad}(X) = \frac{q_{rad}}{2 \;\; \bar{D}^2} \tag{12}$$

Theses relations were obtained by empirical methods.

2.1.3 Conjugated heat flux from liquid side

On the other side, the heat flux produced by combustion is transferred into to cooling jacket. The fuel absorb energy and increases the temperature. For estimate the convective heat flux for the inner wall to fuel the Eq. 13 is used. The subscript letter f refer to fuel.

$$q_f = h_f \;\; (T_x - T_f) \tag{13}$$

Where q_f is the heat flux, h_f convective heat flux coefficient, T_x inner wall temperature on liquid side and T_f fuel temperature.

For the estimate the convective heat transfer coefficient h_f the next dimensionless numbers are define for flow of the fuel in cooling jacket.

Nusselt number:

$$Nu_f = \frac{h_f \;\; d_h}{\lambda_f} \tag{14}$$

Where d_h is the hydraulic diameter and λ_f fuel thermal conductivity.

Reynolds number:

$$Re_f = \frac{\rho_f \ U_f \ d_h}{\mu_f} \tag{15}$$

Where ρ_f fuel density, U_f fuel velocity, and μ_f fuel dynamic viscosity.
Prandtl number:

$$Pr_f = \frac{\mu_f \ c_f}{\lambda_f} \tag{16}$$

Where c_f fuel specific heat.
From the similarity theory:

$$Nu_f = 0.023 \ Re_f^{0.8} \ Pr_f^{0.4} \tag{17}$$

Then the convective heat transfer coefficient can be expressed by Eq. 18:

$$h_f = 0.023 \ \frac{(\rho_f \ U_f)^{0.8} \ c_f^{0.4} \ \lambda_f^{0.6}}{d_h^{0.2} \ \mu_f^{0.4}} \tag{18}$$

The coefficient of ribbing η_r is a relation of the convective heat flux considering the cooling jacket with ribs q_{frib} and without ribs q_f. It is can be calculated by Eq. 19.

$$\eta_r = \frac{q_{frib}}{q_f} \ ; \ \eta_r \approx 2.5 \ in \ practice. \tag{19}$$

2.1.4 Calculation procedure

The first step is define an one-dimensional (1-D) mesh for the combustion chamber contour. For this study was chosen the combustion chamber contour represented on Fig. 5.

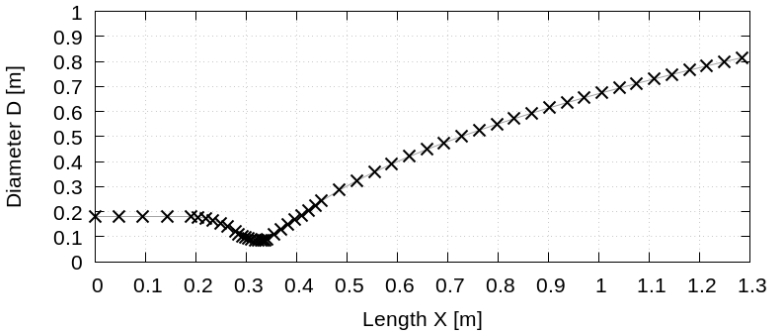

Figure 5. One-dimensional mesh

The mesh sensitivity was studied by varying the number of points along the combustion chamber contour, regions with high gradients of temperature and heat flux were taken into account for distribution of points. Each point has a coordinate X_i for i in interval from 0 to n, where n is the number of points.

Parameters of design of the combustion chamber must be defined for performed semi-empirical calculation. The core temperature $T_k = 3507.2K$ (adiabatic flame temperature), inner wall temperature for hot gas side $T_{ct} = 850K$, mixture ratio on wall layer $\phi = 3$ and chamber pressure $p_k = 6MPa$. The chemical equilibrium for combustion of the ethanol (C_2H_5OH) and oxygen (O_2) was obtained by software *Chemical Equilibrium with Applications* (CEA NASA) and returned the following values for the hot gas mixture.

1. Mass fraction of the combustion products CO, CO_2, H, H_2, H_2O, OH, O_2, respectively:
   $x = [\ 0.35160,\ 0.04840,\ 0,\ 0.44840,\ 0.15160,\ 0,\ 0\ ]$;
2. Ratio of specific heats: $\gamma = 1.25$;
3. Dynamic viscosity: $\mu = 0.53150 \cdot 10^{-4}$;
4. Prandtl number: $Pr = 0.5295$;
5. Hot gas mixture temperature at wall layer: $T_{or} = 1468.47K$;

6. Ideal gas constant: $R = 8.3145\ \ j/mol.K$.

Total heat flux q_{total} from the combustion gases can be obtained calculating the convection heat flux by Eq. 1 and radiation heat flux by Eq. 6, for each point of the mesh, then both vectors are added (Eq. 20). For the first approximation of the total heat flux, the temperature of the wall on the gas side T_{ct} must be adopted, $T_{ct} = 850$ in this study. This approximation too allows us to obtain q_{co1000}, value that we will use in the next steps.

$$(q_{total})_i = (q_{co})_i + (q_{rad})_i \tag{20}$$

For evaluation of the fuel heating in the cooling jacket in each point of the mesh we use Eq. 21 and Eq. 22.

$$(\Delta T_f)_i = \frac{0.5\ \ (q_{total})_i\ \ \Delta S_i}{c_f\ \ \dot{m}_f} \tag{21}$$

$$\Delta T_f = \sum_{i=0}^{n} (\Delta T_f)_i \tag{22}$$

Where $\dot{m}_f$ is the fuel mass flow and S_i is the lateral surface of the combustion chamber at position i and can be obtained by Eq. 23.

$$\Delta S_{i+1} = \left[\left(\frac{D_i + D_{i+1}}{2} \right) \pi \ - n_a E_a \right] \Delta X \tag{23}$$

Where D_i is the combustion diameter at position i, n_a number of ribs, E_a rib thickness and ΔX is the distance from i to $i + 1$.

Then the outlet fuel temperature T_{fout} can be obtained by Eq. 24, inlet fuel temperature T_{fin} added to fuel heating in the cooling.

$$T_{fout} = T_{fin} + \Delta T_f \tag{24}$$

The outlet fuel temperature can not be higher than the fuel vaporization temperature at operation pressure.

Convective heat transfer coefficient can be obtained by Eq. 18, considering $\xi_f = 1$. The velocity of the fuel for each point of the mesh can be obtained by Eq. 25.

$$(U_f)_i = \frac{\dot{m}_f}{\rho_f\ \ (S_s)_i} \tag{25}$$

Where $(S_s)_i$ is the cross section area of the channel at position i.

The next step is estimate new values of the T_{ct} using q_{co1000} and heat flux relations (Eq. 26, Eq. 27 and Eq. 28).

$$\frac{q_{co}}{q_{co1000}} = \frac{T_{or} - T_{ct}}{T_{or} - 1000}\ \ ;\ \ \frac{q_{co800}}{q_{co1000}} = \frac{T_{or} - 800}{T_{or} - 1000}\ \ ;\ \ \frac{q_{co1400}}{q_{co1000}} = \frac{T_{or} - 1400}{T_{or} - 1000} \tag{26}$$

On the other hand:

$$\frac{q'_{co}}{q_{co1000}} = \left[\frac{(T_{ct} - T_f)}{\frac{E_1}{\lambda_w} + \frac{1}{(h_f \eta_r)}} - q_{rad} \right] / q_{co1000} \tag{27}$$

$$\frac{q'_{co800}}{q_{co1000}} = \left[\frac{(800 - T_f)}{\frac{E_1}{\lambda_w} + \frac{1}{(h_f \eta_r)}} - q_{rad} \right] / q_{co1000}\ \ ;\ \ \frac{q'_{co1400}}{q_{co1000}} = \left[\frac{(1400 - T_f)}{\frac{E_1}{\lambda_w} + \frac{1}{(h_f \eta_r)}} - q_{rad} \right] / q_{co1000} \tag{28}$$

Where λ_w is the inner wall thermal conductivity and E_1 inner wall thickness.

These relations calculated at the extremes for $T_{ct} = 800$ and $T_{ct} = 1400$ allows define the functions and make the interpolation according to Fig. 6 for determine new values of T_{ct}.

With the new values of the T_{ct} the vector q_{co} is recalculated by Eq. 1 and q_{total} is updated. This allows us recalculate T_f by Eq. 21 and T_x by Eq. 29.

$$(T_x)_i = (T_{ct})_i - \left(\frac{E_1}{\lambda_w} q_{total} \right)_i \tag{29}$$

This cycle is repeated until T_x stop changing (see Fig. 7). This method proposed by Kessaev (1997) and Vasiliev *et al.* (1993) was implemented in Python language.

The first total heat flux approximation, calculated considering the $T_{ct} = 850$, and the total heat flux calculated after cycle convergence are represented on Fig. 8.

The final values of the convective, radiation and total heat flux are represented on Fig. 9.

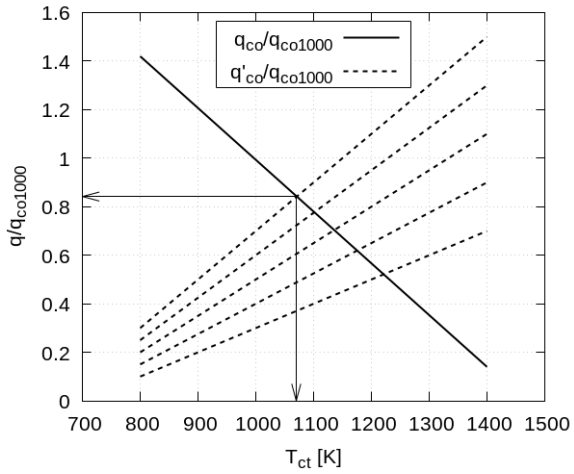

Figure 6. Interpolation to correct the T_{ct} and heat flux.

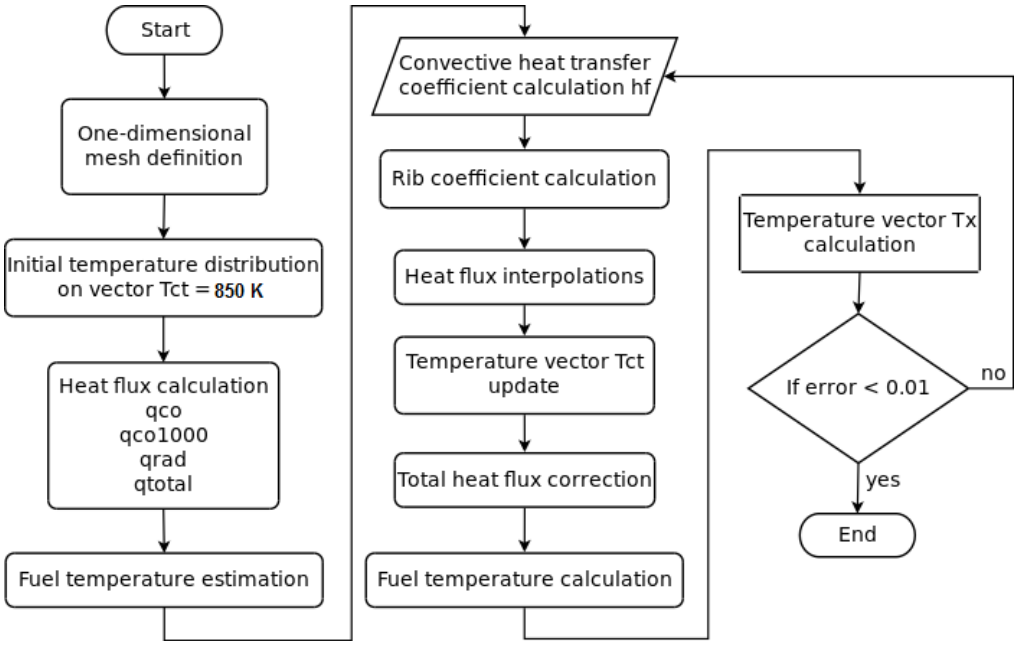

Figure 7. Flow chart for semi-empirical calculation procedure

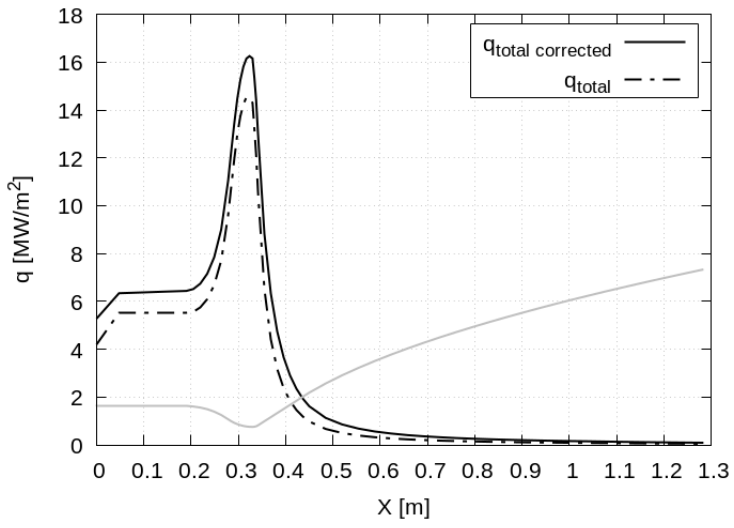

Figure 8. Total heat flux corrected

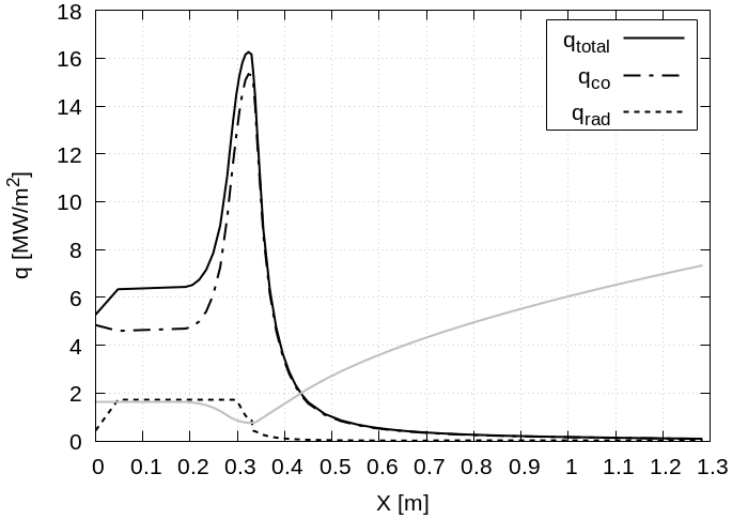

Figure 9. Total heat flux provided by convection and radiation

2.1.5 Semi-empirical calculation correction

Defining a correction factors relating semi-empirical temperatures with CFD temperatures.

$$\xi_f = \frac{T_f}{(T_f)_{cfd}} \tag{30}$$

$$\xi_x = \frac{T_x}{(T_x)_{cfd}} \tag{31}$$

$$\xi_{ct} = \frac{T_{ct}}{(T_{ct})_{cfd}} \tag{32}$$

These coefficients can be used to adjust semi-empirical calculation.

2.1.6 Pressure losses

The total pressure losses in the cooling jacket can be estimated by Eq. 33 and is the sum of the friction and local loses for each point of the mesh.

$$\Delta p_f = \sum_{\Delta X_i} (\Delta p_{1i} + \Delta p_{2i}) \tag{33}$$

Where Δp_{1i} is the friction losses and Δp_{2i} is the local resistance losses for a point i of the mesh.
The friction losses can be calculated by Eq. 34.

$$\Delta p_{1i} = \xi_{f1} \frac{\Delta X_i}{d_h} \frac{\left(\rho_f U_f^2\right)_i}{2} \tag{34}$$

The friction losses coefficient depend of the Reynolds number and can be calculated by Eqs. 35 and 36
For Re = $3.10^5 \sim 10^5$ can be calculated by:

$$\xi_{f1} = \frac{0.3164}{Re^{0.25}} \tag{35}$$

For Re = $10^5 \sim 10^8$ can be calculated by:

$$\xi_{f1} = 0.0032 + \frac{0.221}{Re^{0.237}} \tag{36}$$

The local resistance losses can be calculated by Eq. 37.

$$\Delta p_{2i} = \xi_{f2} \frac{\left(\rho_f U_f^2\right)_i}{2} \tag{37}$$

Where $\xi_i = 0.01$ is the local resistance coefficient adopted in this work.

Total and static pressure relation:

$$p_{total} = p_{stc} + \frac{\rho_f U_f^2}{2} \tag{38}$$

2.2 Computational fluid dynamics

Computational fluid dynamics were performed take into account the total heat flux obtained from semi-empirical calculation as boundary condition according to Fig. 9.

The turbulence model $k - \omega$ was used in this simulation due to the robustness, computational cost and the treatment of the equations for flow near the wall. The *OpenFOAM 5.0* software was used to CFD modelling and the solver *chtCustomMultiRegionSimpleFoam*, which in turn has the steady-state *SIMPLE* (Semi-Implicit Method for Pressure Linked Equations) numerical solution method.

2.2.1 Governing equations and numerical method

The governing equations were defined taking into account the follow simplifying hypotheses:

1. Steady state flow;
2. Incompressible fluid;
3. There are not body forces;
4. Thermophysical properties for cooling are constants, dynamic viscosity (μ), density (ρ), fuel thermal conductivity (λ_f) and specific heat (c_p);
5. Thermal conductivity for walls (λ_w) are constants.

Conservation of mass equation:

$$\nabla\cdot(\rho\vec{u}) = 0 \tag{39}$$

Conservation of momentum equation:

$$\nabla\cdot(\rho\vec{u}\vec{u}) = -\nabla p + \nabla\cdot\tau \tag{40}$$

Total energy conservation equation for liquid regions:

$$\nabla\cdot(\rho\vec{u}E) = -\nabla\cdot(p\vec{u}) + \nabla\cdot(\tau\cdot\vec{u}) - \nabla\cdot q \tag{41}$$

Energy equation for solid regions:

$$\nabla\cdot q = 0 \tag{42}$$

Where $\vec{u}$ is velocity vector, p pressure, τ viscous stress tensor, E total energy and q heat flux.

Making the decomposition of the momentum conservation equations Eq.(40) by Reynolds mean, considering an average velocity ($\vec{U}$) added to a fluctuation (u') Eq.(43), the viscous stress tensor takes the form of Eq.(44) (Tennekes and Lumley, 1972).

$$\tilde{u} = \vec{U} + u' \tag{43}$$

$$\tau = \mu\nabla\vec{U} - \overline{\rho u'u'} \tag{44}$$

Making the same decomposition the energy conservation equations Eq.(41) by Reynolds mean, considering an average temperature (Θ) added to a fluctuation (θ') Eq.(45), the heat flux takes the form of Eq.(46) (Tennekes and Lumley, 1972).

$$\tilde{\theta} = \Theta + \theta' \tag{45}$$

$$q = -\left(\lambda\nabla\Theta - \overline{\theta'u'}\right) \tag{46}$$

The Reynolds tress $\overline{\rho u'u'}$ and $\overline{\theta'u'}$ should be modeled to describe the turbulent problem. In this work the closing of the equations is obtained using the turbulence closure model $k - \omega$ and are presented in Wilcox (1993).

The initial conditions for k and ω at inlet, were estimated by the follow relations:

$$k = \frac{3}{2}\left(I_t \mid \vec{u_0} \mid\right)^2 \tag{47}$$

$$\omega = \frac{k^{0.5}}{d_h 0.09^{0.25}} \tag{48}$$

Where k turbulence kinetic energy and ω dissipation of the turbulence kinetic energy, $\vec{u_0}$ inlet velocity and I_t is turbulence intensity was considered $I_t = 0.2$.

2.2.2 Mesh data

Mesh sensitivity was tested by varying the number of elements and comparing them with the numerical calculation responses, until maximum temperatures show stability. All studies were carried out on the same configuration hardware, using 12 nodes each with 16 *Intel Xeon* 2.6 GHz CPUs and 64 Gb memory per node. The properties of the tested meshes are given in Tab. 1.

Dimensionless parameter y^+ can be estimated Eq.(49). For good approximation of the boundary layer first computation node should be located at $y^+ \leq 5$ (Denies, 2015).

$$y^+ = \frac{u_* y}{\nu} \tag{49}$$

Table 1. Meshs data.

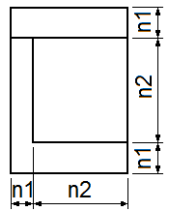	n1$^{(1)}$	n2$^{(1)}$	Number of nodes	Number of interactions	Mesh first node [μm]	y^+ [min-max]	Processing time [h]
Mesh	20	50	7,676,860	254,997	40.8	2.04e-3 $\sim$ 8.25	9.15

$^{(1)}$ Number of divisions in geometry

3. RESULTS

The solution was considered converged when the residual of the energy equation reached 10^{-7}. From this limit the temperature variations are of the order 10^{-2} and become depressible. Figure 10 shows the evolution of the residual.

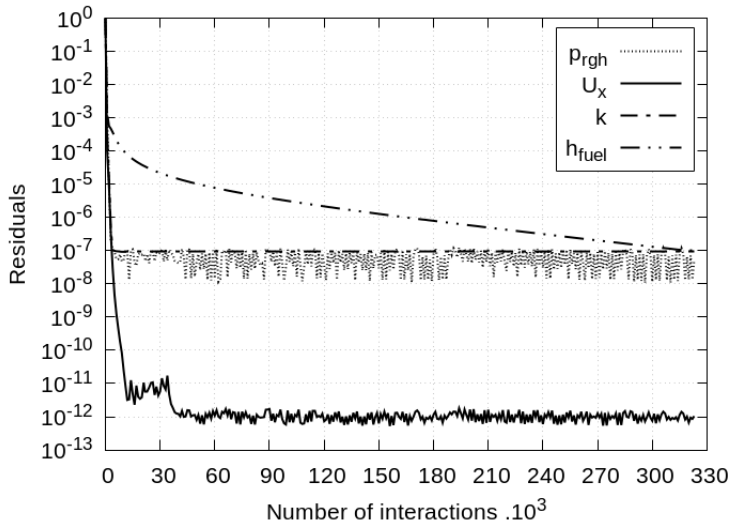

Figure 10. Residuals for CFD modeling

The root-mean-squared error (RMS) was estimated by following relation (Eq. 50).

$$RMS = \sqrt{\frac{\sum_{i=1}^{j} (x_{1i} - x_{2i})^2}{j}} \tag{50}$$

Where x_{1j} and x_{2j} are the values to be compared. For this study was considered the distribution of 54 points along the cooling jacket to collect theses values according to 1-D mesh (Fig. 5).

The inner wall temperature on gas side for CFD model and semi-empirical calculation can be seen in Fig. 11.

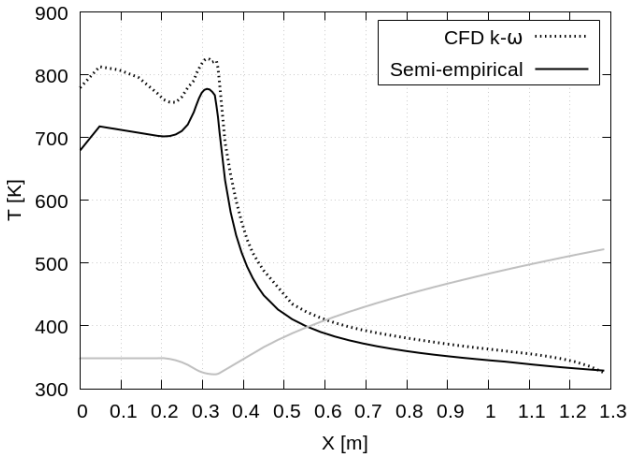

Figure 11. Internal wall temperature of the gas side

Comparing semi-empirical and CFD for inner wall temperature on gas side the RMS result is $47.77\ K$.
The inner wall temperature on liquid side for CFD model and semi-empirical calculation can be seen in Fig. 12.

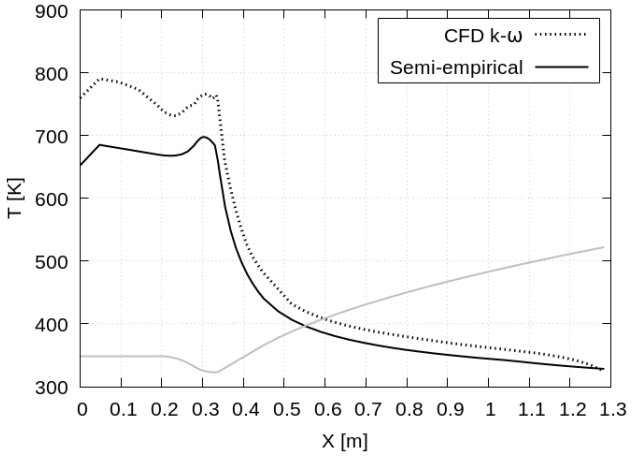

Figure 12. Internal wall temperature of the liquid side

Comparing semi-empirical and CFD for inner wall temperature on liquid side the RMS result is $57.22\ K$.
The fuel temperatures for CFD model and semi-empirical calculation are available in Fig. 13.

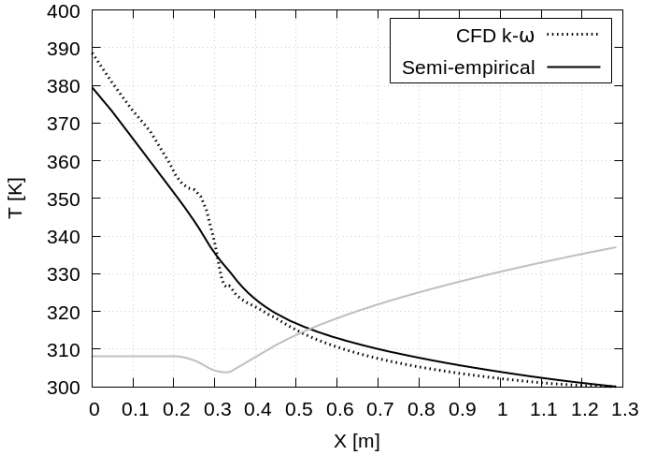

Figure 13. Fuel temperatures in cooling jacket

Comparing semi-empirical and CFD for fuel temperatures the RMS result is $4.09\ K$.

The module of velocities for CFD model and semi-empirical calculation are available in Fig. 14.

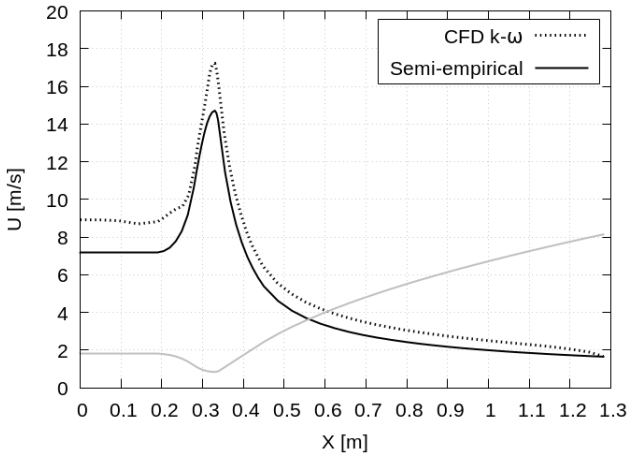

Figure 14. Velocity magnitude of the fuel in cooling jacket

The differences found between CFD models and semi-empirical calculation are justified by not considering the turbulence. Comparing semi-empirical and CFD for velocity magnitude the RMS result is $1.37\ m/s$.

The total pressures for CFD and semi-empirical calculation are available in Fig. 15.

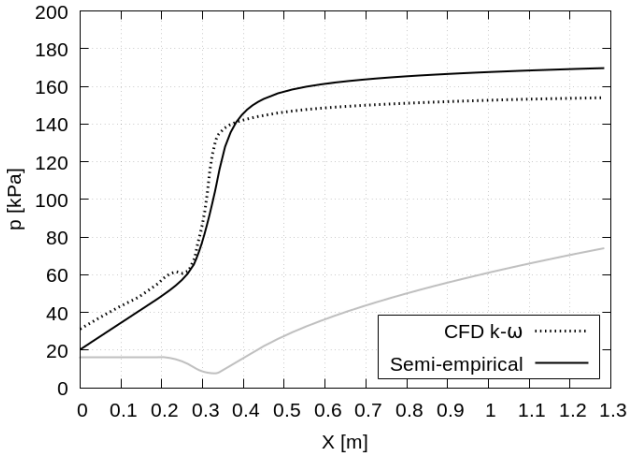

Figure 15. Pressure drop

It is observed the greater proximity between the values and the RMS result is $1.34\ kPa$.

The distribution of the correction factors defined according to Eq. 30, Eq. 31 e Eq. 32 can be seen in Fig. 16.

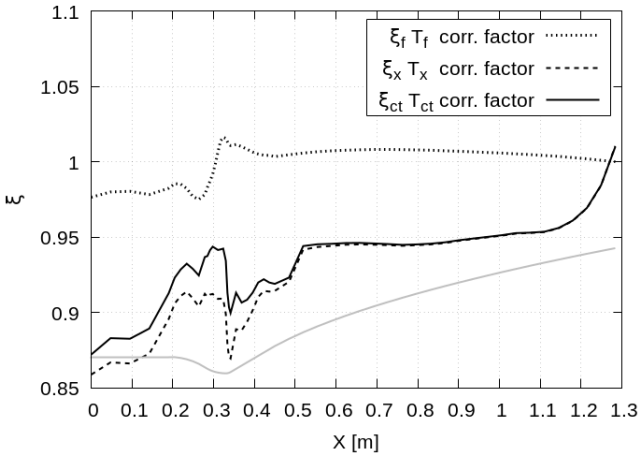

Figure 16. Correction factors

The temperature values in the cross section of the throat and outlet regions of the cooling jacket were obtained for the solid and liquid domains. The results can be seen in Fig. 17.

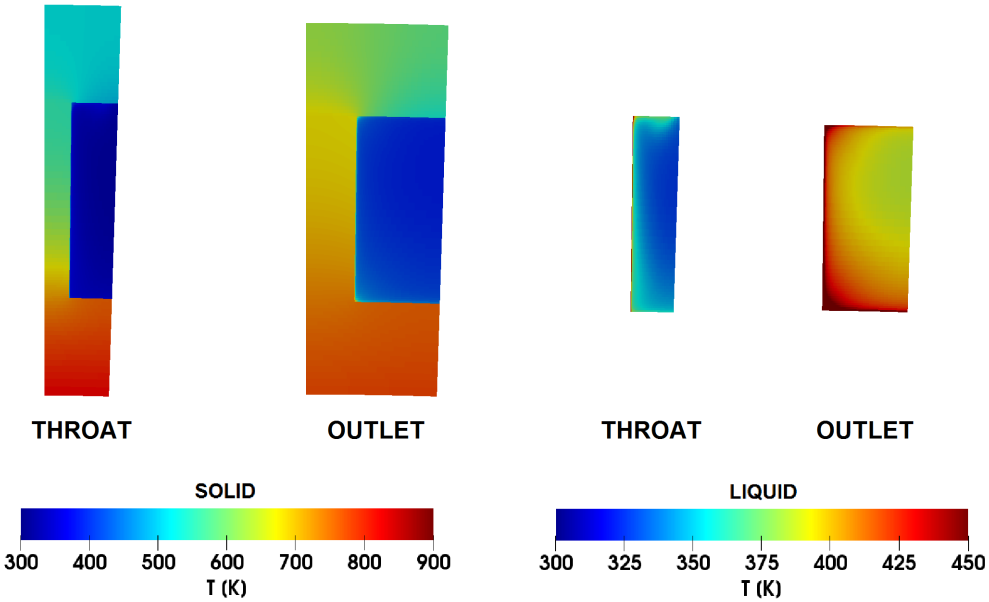

Figure 17. Temperature distribution on the throat section

4. CONCLUSIONS

With theses results on the hand, it can be note that the profile of the temperatures, pressure loss and velocity along the chamber is similar for both semi-empirical and CFD calculations. The next step was adjust semi-empirical calculation, determining the correction coefficients ξ. This correction allows us to obtain the fast tool of the analysis for cooling jacket applied on liquid propellant rocket engine by a semi-empirical method.

The continuity of this work may be to develop an experimental method where it will be possible to measure the temperatures and pressure loss of the fuel for a well defined channel and geometry. The acquisition of these data will allow us to determine if CFD model will have the best results for a real application and will also allow us to adjust the semi-empirical calculation definitively.

5. ACKNOWLEDGEMENTS

The first author acknowledges the CAPES for financial support to undergraduate student and IAE-APE for the space ceded.

6. REFERENCES

Denies, L., 2015. *Regenerative Cooling Analysis of Oxygen Methane Rocket Engines*. Master's thesis, Delft University of Technology.

Kessaev, J.V., 1997. *Theory and calculation of liquid-propellant engines*. MAI (Moscow Aviation Institute).

Kurpatenkov, V., Berezaya, E., Kudryavtseva, L. and Cradle, L., 1989. *Calculation of radiant heat fluxes*. Moscow Aviation Institute.

NASA, 1972. "Liquid rocket engine fluid-cooled combustion chambers". Space vehicle design criteria SP-8087.

Sutton, G.P. and Biblartz, O., 2001. *Rocket Propulsion Elements*. John Wiley & Sons, 7th edition.

Tennekes, H. and Lumley, J.L., 1972. *A first course in turbulence*. The MIT Press, Massachusetts.

Vasiliev, A., Kudryavtsev, V., Kuznetsov, V., Kurpatenkov, V., Obelntsky, A., Polyaev, V. and Poluyan, V.Y., 1993. *Fundamentals of Theory and Calculation of Liquid Fuel Rocket Engine*, Vol. 2. Pererab, 4th edition.

Wilcox, D.C., 1993. *Turbulence Modeling for CFD*. DWC, Industries, Inc.

7. RESPONSIBILITY NOTICE

The authors are the only responsible for the printed material included in this paper.